Master's Thesis

Cell entry and early infection of Echovirus 30

Tino Kantoluoto

University of Jyväskylä

Department of Biological and Environmental Science

Cell and Molecular Biology

23.05.2020

UNIVERSITY OF JYVÄSKYLÄ, Faculty of Mathematics and Science
Department of Biological and Environmental Science
Cell and Molecular Biology

Kantoluoto Tino V. V. Cell entry and early infection of Echovirus 30
MSc thesis: 43 p.
Supervisors: Adj. Prof. Varpu Marjomäki and Prof. Michael Lindberg
Reviewers:
May 2020

Keywords: CAR, DAF, Endosome, Enterovirus, purification

Enteroviruses are small, non-enveloped positive sense RNA viruses that primarily target the epithelial cells of the gastrointestinal tract, but are known to cause variety of clinical complications in secondary tissues. Echovirus 30 (E30) is a member of the enterovirus B genus and it causes epidemic bursts of aseptic meningitis all around the world. Despite being a common agent for this neurological disease, not much is known of E30 biology. Here, we have purified E30 and studied its cell entry and early infection using confocal microscopy and receptor binding assay. Some enterovirus B species are known to utilize decay accelerating factor (DAF) and coxsackie and adenovirus receptor (CAR) for cell entry and E30 has also previously been reported to use DAF for its infection. Here, we performed a receptor binding assay using radioactive E30 and showed that E30 indeed binds to DAF, but does not have any affinity towards CAR. Co-localization analyses performed from confocal images with various immunolabeled cell markers showed that E30 is not using the clathrin mediated pathway for its internalization, but still enters the early and late endosomes during infection. Localizing in these endosomal structures is not very common among members of enterovirus B species, apart from echovirus 7 (E7), which is another DAF-but-not-CAR binding virus. E30 showed rapid kinetics for its infection cycle, as genome replication was observed to start already after 2.5 h of infection. Modifications in the host cell endoplasmic reticulum were also observed already at 2 h p.i.. These findings of E30 early infection guide the following research to the right way and makes a connection between E30 and E7 behavior.

JYVÄSKYLÄN YLIOPISTO, Matemaattis-luonnontieteellinen tiedekunta
Bio- ja ympäristötieteiden laitos
Solu- ja molekyylibiologia

Tino Kantoluoto Echovirus 30:n soluun sisäänmeno ja infektion alkupuolen tapahtumat
Pro gradu -tutkielma: 43 s.
Työn ohjaajat: Dos, FT, Varpu Marjomäki ja Prof. Michael Lindberg
Tarkastajat:
Toukokuu, 2020

Hakusanat: CAR, DAF, Endosomi, Enterovirus, Puhdistus

Enterovirukset ovat pieniä ja vaipattomia positiivisen RNA genomin omaavia viruksia, jotka infektoivat pääasiassa ruoansulatuskanavan epiteelisoluja, mutta voivat muihin kudoksiin levitessään aiheuttaa erilaisia sairauksia. Echovirus 30 (E30) kuuluu enterovirusten B ryhmään ja aiheuttaa aivokalvontulehdus-epidemioita ympäri maailmaa. Huolimatta virulenttiudestaan, E30:n perusbiologiasta tiedetään toistaiseksi hyvin vähän. Tässä Pro Gradu -tutkielmassa puhdistettiin E30:tä ja tutkittiin sen soluun sisään menoa ja infektion alkupuolen tapahtumia. Osan enterovirus B -ryhmän jäsenten tiedetään käyttävän ”Decay accelerating factor” (DAF) -proteiinia sekä coxsackie- ja adenovirusreseptoria (CAR) soluun tunkeutuessaan. DAF:n on aiemmin osoitettu olevan tärkeä solun tekijä E30:n infektiossa. Tässä tutkielmassa osoitettiin radioaktiivisella reseptorisitoumis- kokeella että E30 sitoutuu DAF:iin, mutta ei lainkaan CAR:iin. Konfokaalimikroskopiakuvista tehdyt kolokalisaatioanalyysit osoittivat, että E30 ei käytä klatriinivälitteistä endosytoosireittiä, mutta siirtyy silti infektion edetessä aikaisiin ja myöhäisiin endosomeihin. Tyypillisesti enterovirus B ryhmän jäsenet eivät esiinny näissä solurakenteissa, lukuun ottamatta echovirus 7:ää (E7), joka myös on DAF:iin, mutta ei CAR:iin, sitoutuva enterovirus. E30-infektion osoitettiin myös etenevän nopeasti, sillä sen RNA-genomi alkoi replikoituimaan jo 2,5 tunnin jälkeen. Myös isäntäsolun solulimakalvostossa osoitettiin tapahtuvan muutoksia jo 2 tunnin jälkeen. Nämä tulokset tuovat tärkeää tietoa E30-infektion kulusta ja osoittavat samankaltaisuuksia E30:n ja E7:n välillä.

TABLE OF CONTENTS

TERMS AND ABBREVIATIONS

CAR	Coxsackie and adenovirus receptor
CD63	Tetraspanin CD63
CI-MPR	Mannose 6-phosphate receptor
CVA9	Coxsackievirus B9
CVB3	Coxsackievirus B3
DAF	Decay accelerating factor
DMEM	Dulbecco's Modified Eagle Medium
dsRNA	double stranded RNA
E1	Echovirus 1
E7	Echovirus 7
E30	Echovirus 30
EEA1	Early endosome antigen 1
MOI	Multiplicity of infection
p.i.	Post-infection
RD cells	Human Rhabdomyosarcoma cells
TEM	Transmission Electron Microscope

1 INTRODUCTION

1.1 Enteroviruses

Enteroviruses are small, ~30nm in diameter, non-enveloped viruses, that belong to a *Picornaviridae* family. The genus *Enterovirus* itself is further divided into 12 different species of viruses (EV A-J and Rhinovirus A-C), with species EV A, -B, -C, -D and Rhinoviruses A, -B and -C found in humans (Nikonov et al. 2017).

Most of the enterovirus infections in humans go unnoticed, but they can cause wide range of different diseases, with symptoms ranging from common cold type illness to neurological syndromes and inflammation of secondary tissues, such as different types of skin rash, myocarditis, hand-foot-and mouth disease and acute hemorrhagic conjunctivitis (Roivanen et al. 1998, Fields et al. 2013, Nikonov et al. 2017). The most studied and well known enterovirus is the poliovirus from enterovirus C species, the major agent causing poliomyelitis that lead to death and crippling of thousands of people back in 20th century and before. Effective vaccination campaign against polio was started in 1988 in order to eradicate it completely and since then, paralytic poliomyelitis cases have decreased by over 99% (Bandyopadhyay et al. 2015). This fight against polio made way for the study of other enteroviruses also and shed lots of light on basic biology of these viruses.

Enteroviruses have a ~7500 nucleotide sized single-stranded, positive sense RNA genome, that encodes for a single polyprotein. (Nikonov et al. 2017). This polyprotein is cleaved at designated sites to structural and non-structural proteins, with many of the intermediate proteins serving a function as well. The precursor protein P1 region of the polyprotein contains structural proteins VP1, VP2 and VP3 that form outer surface of the icosahedral capsid and VP4 that functions as an internal structural protein (Tuthill et al. 2010, Nikonov et al. 2017). P2 and P3 precursor protein regions contain the non-structural proteins, which have multiple

functions relating to viral replication, polyprotein cleaving and host immune response evasion (Laitinen et al. 2016, Nikonov et al. 2017).

1.2 Enterovirus life cycle

As enteroviruses spread mostly via fecal-oral manner, they primarily target the endothelium cells of the gastro-intestinal tract and can spread from there to cause clinical complications and diseases in secondary target tissues (Wells and Coyne 2019). Life cycle of enterovirus species (Figure 1.) begins at the cell membrane of the host cell, where they initiate their entry by triggering an endocytosis by attaching to cell membrane receptor proteins. Some enterovirus species, such as Coxsackievirus B3 (CVB3), need to utilize two different receptors for an efficient infection (Coyne and Bergelson, 2006). Furthermore, different viruses can trigger various different endosomal pathways with various receptors.

After internalization, virus particles reside inside the endosomes and start to undergo an uncoating process, during which the viral RNA is released to the cytoplasm. Receptor binding, exposure to acidic environment or some other trigger inside endosomes causes the native enterovirus particle to go through set of conformational changes, resulting in what is known as an intermediate particle, or the activated particle (A-particle). Although the cause for this transition varies among species, the changes that the particles go through remain similar: particle diameter increases, VP4 subunits are lost and the N-termini of VP1 capsid proteins are exposed outside the particle (Fricks and Hogle 1990, Tuthill et al. 2010, Ren et al. 2013). Although virus genome does not leave the particle immediately when the A-particle is formed, some changes in RNA-capsid interactions have been shown (Pickl-Herk et al. 2013, Organtini et al. 2014). Recently, it has been shown with echovirus 18 (E18) and echovirus (E30), that during RNA egress, the viral capsid loses up to three capsid pentamers in order to let the genome exit the capsid (Buchta et al. 2019).

After the viral genome is released into the cytosol, the viral RNA is translated by the host cell ribosome machinery into a single polyprotein, which is further cleaved into functioning proteins. One of these cleaved proteins is the RNA-dependent RNA polymerase 3D ($3D^{pol}$), which initiates the viral replication by synthesizing a negative-stranded replica of the positive-stranded viral genome (Wu et al. 2010, Wells and Coyne 2019). This negative-stranded RNA is then used as a template for synthesis of new positive-sensed genomes, which further again are used in translation of the polyprotein, creation of new negative sense RNA genomes or ultimately are packaged into new viral particles. Double stranded RNA (dsRNA) is formed as an intermediate product during the RNA replication. During this replication process, host cell membrane structures are altered to create so called replication organelles (RO), where the viral replication mainly takes place (van der Schaar et al. 2016). It has been thought that these ROs serve to concentrate the viral and host proteins required for replication, but also to protect the virus from cellular RNAses and other antiviral machinery (van der Schaar et al. 2016).

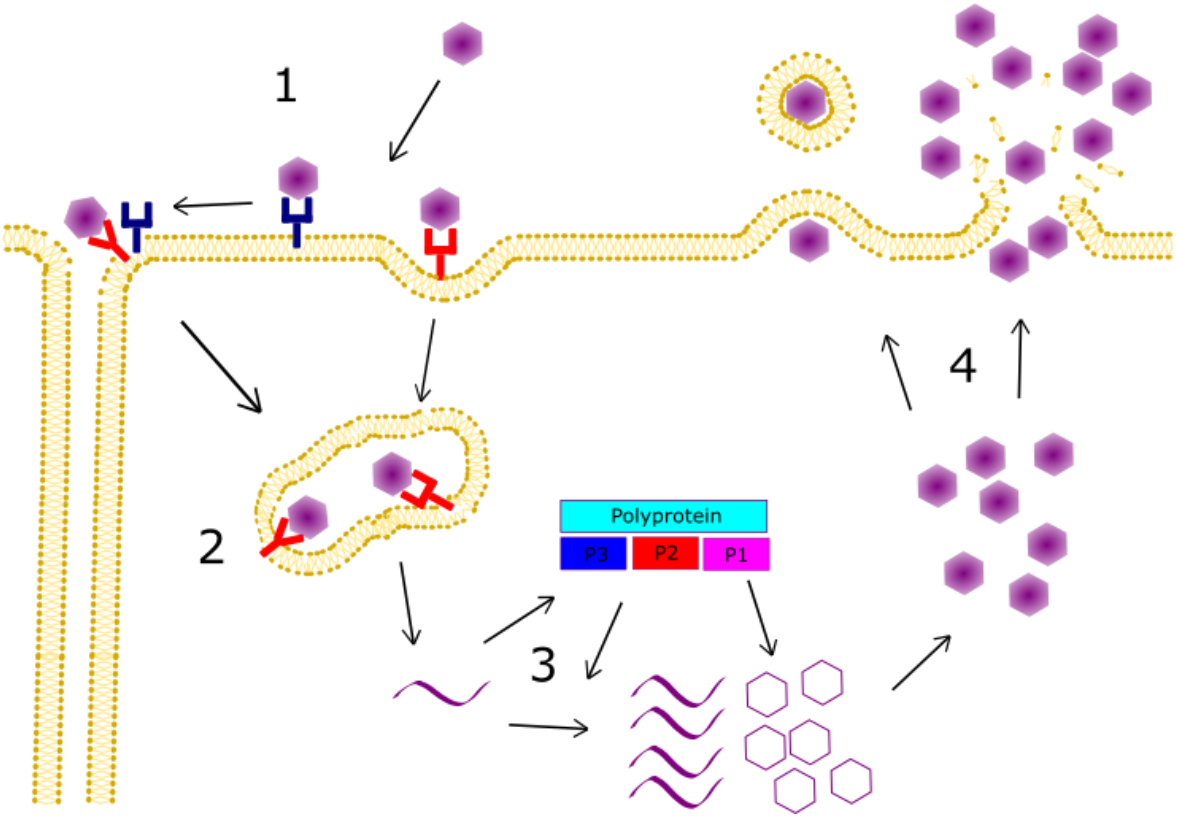

Figure 1. Enterovirus life cycle. Enterovirus enters the cell by attaching to a receptor and activating an endocytosis. (1) Some viruses, such as CVB3, require two receptors, of which the first functions as an attachment receptor that transfers the virion to its main receptor. Inside the cell, virions localize inside endosomal structures and begin their uncoating phase, during which the virus genome exits from the capsid and is released into the cytosol (2). In the cytosol, the viral genome is translated by host cells' ribosomal machinery into a single polyprotein, that is cleaved into functional proteins (3). Proteins cleaved from the P3 and P2 region participate in replication of RNA and alter the host cell functions to facilitate the infection. P1 region contains the capsid proteins for new viral particles, which are filled with the new RNA copies. Once the new virions have been assembled, they exit the host cell mainly by lysing it and bursting out, but in some instances virions can also exit in a non-lytic manner inside host cell membrane derived vesicles (4).

After sufficient viral replication and accumulation of new enteroviral virions, virus exits the cell to infect other nearby cells. The exit has traditionally been thought to happen only via cellular lysis, where the whole cell breaks down and all new virions are released simultaneously (Fields et al. 2013). This model has been challenged in recent years, however, as few studies have provided evidence also for non-lytic exit of the enterovirus virions, in which virion or group of virions exit the cell in host cell membrane derived vesicles (Feng et al. 2013, Chen et al. 2015, Too et al. 2016). This "new" way of spread of these viruses could make us rethink some aspects of the viral entry and early stages of infections as well and could possibly shed more light to understanding some enterovirus borne diseases.

It remains to be studied more in the future, however, whether this non-lytic exit pathway is universal for all enteroviruses or if it is only a virus strain or host cell-type specific attribute.

1.3 Echovirus 30 and Species B enterovirus

Subject of this Master's thesis is the E30 and the early stages of its infection. E30 is a species B enterovirus, a subgroup of enteroviruses that includes more than 30 serotypes of echoviruses (E1 – E7, E9, E 11 – E21, E24 – E27, E29 – E33), six serotypes of coxsackie B viruses (CVB1-6), one coxsackie A virus (CVA9), one simian enterovirus (SA5) and over 20 enterovirus-B (EV-B) serotypes (Nikonov et al. 2017). E30 is best known for causing outbreaks of viral aseptic meningitis worldwide. Several cases throughout the years have been reported from Asia (Zhao et al 2005, Choi et al. 2010, Yang et al. 2013), Europe (Faustini et al. 2006, Holmes et al. 2016), North America (Begier et al. 2008) and Brazil (Pinto Junior et al. 2009). There was also an outburst in western Finland in 2010-2011, with 106 confirmed E30 cases reported (Österback et al. 2015). E30 has been divided into three groups (1-3) already back in late 1960's based on its antigenic heterogeneity (Wenner et al 1967, Duncan 1968) and this heterogeneity has been later studied further with phylogenetic analysis of VP1, VP4/VP2 and VP1/2A genomic regions (Savolainen et al 2001, Künkel et al 2001). Palocios et al. (2002), however, proposed a new classification of E30 epidemiology in an analysis of 318 different strains of E30, where they found two major broad genotypes that are further divided into subgroups and individual strains. They also described E30 to have a molecular epidemiology more similar to influenza virus, where only one lineage at a time circulates the world. This is noted as an unusual behavior for enteroviruses and explains the epidemic nature of E30 (Palocios et al. 2002).

Despite E30 being a major cause for viral aseptic meningitis, not much is still known of its biology or way of infection. Interest towards E30 has increased in recent years, however, and studies have begun to unravel details of E30

interactions with the host cell. As a lot more is known of other members of enterovirus B species, a lot of research has been based on finding similarities and differences in the behavior between E30 and other enterovirus B species members.

1.4 Enterovirus B entry receptors

Common identified cell membrane receptors for Enterovirus B species are Integrin $\alpha_2\beta_1$ for E1 (Bergelson et al. 1992), coxsackie- and adenovirus receptor (CAR) for CVB1-6 (Bergelson et al. 1995, Martino et al. 2000), decay accelerating factor (DAF) for CVB1, CVB3, CVB5 and various echoviruses (Bergelson et al. 1994, Powell et al 1998) and Neonatal Fc-receptor (FcRn) for various echoviruses (Morosky at al. 2019). DAF has been found to be part of E30 infection also (Powell et al 1998, Zhao et al. 2019). It is important to note, that although DAF is a common receptor among enterovirus B species, it usually doesn't work as an internalization triggering receptor itself, but rather serves as an attachment receptor which the virus uses to gain access to its actual primary receptor. Well described example of such dynamic is CVB3 using DAF to gain access to CAR (Coyne and Bergelson, 2006).

1.4.1 Coxsackie- and adenovirus receptor

CAR is the main uncoating receptor for coxsackie B viruses and an attachment receptor for number of adenovirus serotypes (Hidaka et al 1995, Bergelson et al. 1997, Roelvink et al. 1998, Martino et al. 2000). CAR is a 46-kDA sized integral membrane protein found in tight junctions (TJ) between adjacent cells, where it promotes cell adhesion and works as a restricting barrier to control the paracellular movement of water, ions and other molecules (Cohen et al. 2001). CAR is expressed in various cells types and tissues, such as neurons, endothelial and epithelial cells and it has a critical role in development of cardiomyocytes, central nervous system and lymphatic vasculature during embryonic development (Asher et al. 2005). CAR localization in the TJs poses a challenge for viruses, as

despite CVBs have great affinity towards CAR (Goodfellow et al. 2005), integrity of the tight junctions makes CAR inaccessible and inhibits CVB infection very effectively (Cohen et al. 2001).

1.4.2 Decay Accelerating Factor

DAF (also known as CD55) is used by coxsackie viruses as a binding receptor that transfers the virus to the CAR and is known to be a binding target for many echoviruses as well, including E30 (Bergelson et al., 1994 Powell et al. 1998, Zhao et al. 2019). DAF is a 70 kDa sized glycosylphosphatidylinositol (GPI)-anchored protein found often in lipid rafts on apical surface of polarized cells. In a study conducted with CVB3 infecting polarized intestine endothelial cells, virus binding to DAF caused receptor clustering to the lipid rafts and later initiated a remodeling of actin cytoskeleton by activation of Abl and so further triggering Rac1 (Coyne and Bergelson, 2006). This actin remodeling caused lateral movement of the CVB3-DAF-complexes on the cell surface to tight junctions and made so CAR accessible to the virus. Similar receptor clustering and re-localization to TJ was also shown to be induced by anti-DAF antibody mediated activation. Lateral movement of a DAF-virion complex to the tight junctions has also been reported to happen in E11 binding (Sobo et al. 2011). For CVB3, DAF binding was also shown to activate Fyn, a Src-kinase family member protein, resulting in phosphorylation of caveolin-1 and accumulation of this phosphorylated caveolin-1 to TJ (Coyne and Bergelson, 2006). Within 60 min post infection (p.i.), CVB3 was shown to colocalize in the cytoplasm with caveolin-1 containing vesicles. Interestingly however, CAR was not internalized with the virus.

Cell membrane lipid rafts and their integrity have been shown to be critical for lateral movement of DAF. Previously, it has been shown that perturbation of lipid rafts causes inhibition of GPI-anchored protein clustering (Friedrichson and Kurzchalia, 1998). This same was shown to be true also for DAF; perturbed lipid

rafts prevented DAF-clustering and inhibited CVB3 infection greatly (Coyne and Bergelson, 2006). Lipid rafts and their function are considered as important factor for enterovirus B members in general, as many of the used receptors and internalization factors are associated with them (Marjomäki et al. 2015).

1.5 Cell entry and endosomal compartments

After the cell entry, viruses reside inside endosomal vesicles whose qualities are thought to be dependent on the used receptor and entry pathway. Maybe the most classical and well known receptor mediated entry pathway is the clathrin pathway, where new forming vesicles are coated with clathrin cage (Mercer et al. 2010, Doherty and McMahon 2009). These vesicles move to early endosomes, which later maturate into late endosomes and ultimately into lysosomes. Clathrin mediated endocytosis is used by many viruses as a mean of a cell entry (Mercer et al. 2010), but the members of enterovirus B group are shown in many cases to rely on other paths, such as caveolin-1 dependent pathway (Marjomäki et al. 2015). Caveolae are cholesterol rich lipid rafts that form flask shaped invaginations of the cell membrane, that can pinch off and form endosomal vesicles (Doherty and McMahon 2009). Caveolin-1 is a protein found in many non-muscle cells needed for formation of these caveolae and it is commonly used as a marker for caveolae dependent endocytic pathway (Doherty and McMahon 2009). Enteroviruses can utilize also other endocytic pathways, such as micropinocytosis, or viruses can also trigger some new endocytic pathways.

1.5.1 Coxsackievirus B3

As described previously, CVB3 enters the polarized human intestinal cells (Caco-2 to be exact) in caveolin-1 associated vesicles (Coyne and Bergelson, 2006). Role of the caveolin-1 was reported to be critical, as CVB3 cell entry and infection was greatly inhibited in cells transfected with a dominant-negative caveolin-1 mutant

(Coyne and bergelson, 2006). On the other hand, blocking of clathrin mediated endocytosis pathway was reported not to affect the infection rate in any way, strongly indicating that CVB3 is not associated with clathrin mediated pathway and rather utilizing the caveolin-1 dependent pathway. CVB3 has not been associated with any common clathrin pathway markers of early or late endosomes either (Coyne and Bergelson, 2006, Marjomäki et al. 2015). It is currently unclear, that in what endosomal structures CVB3 resides during its early infection. It has been shown however, that CVB3 does not require acidification for its infection (Patel et al. 2009).

As a great contradiction to previous information, in a study conducted with HeLa cells, CVB3 was reported to require CAR for infection, but also to colocalize with clathrin during the internalization and was later found associated with early endosome marker EEA1 (Chung et al. 2005). Endosomal acidification was also found to be required for the CVB3 proliferation (Chung et al. 2005). This opposing information shows the challenges of studying enteroviral infection pathways, as viruses can have varying behavior in different cell types.

1.5.2 Echovirus 1

E1 uses the integrin $\alpha_2\beta_1$ as its receptor and it has not been associated with any markers of clathrin mediated pathway or classical lysosomal pathway (Bergelson et al. 1992, Marjomäki et al. 2015). E1 binding initiated endocytosis has not been observed to follow the normal recycling pathway of integrin $\alpha_2\beta_1$ either, but rather to be a new non-recycling and calpain dependent degradative route for integrin $\alpha_2\beta_1$ (Rintanen et al. 2012). E1 has been associated with caveolins, but the interactions have been observed to happen during first minutes of infection, suggesting that internalization is on not happening in caveolin-1 mediated endosomes (Karjalainen et al. 2008). Any definitive marker for E1 entry has not yet been recognized (Marjomäki et al. 2015). It has been observed, however, that endosomal structures where the E1 and integrin $\alpha_2\beta_1$ accumulate, turn into

multivesicular bodies (MVBs) with intraluminal vesicles inside them during the infection (Karjalainen et al. 2008). Permeability of these MVBs has been shown to increase 1 to 3 hours p.i. and it has been thought to facilitate the viral genome egress in to the cytosol (Soonsawad et al.2014). This increase in permeability might by caused by the VP4 ability to induce pores to membrane structures (Panjwani et al. 2014). Although not all is known of the function and nature of the these MVB structures, it is known for high certainty that the infectious route that E1 uses is not acidifying during infection (Karjalainen et al. 2008, Pietiläinen et al. 2004, Karjalainen et al. 2011)

1.5.3 Coxsackievirus A9

In human lung carcinoma cells (A549), CVA9 has been shown not to require clathrin or caveolin-1 for its cell entry, but rather utilize integrin αVβ6, β2-microglobulin, dynamin and Arf6 in its endocytic pathway (Heikkilä et al. 2010). Interestingly, although CVA9 requires integrin αVβ6 for its infection, αVβ6 is actually not internalized with the virus. Internalization pathway was also separated from common integrin endocytic pathway in general, as small interfering RNA (siRNA) silencing of common integrin-signaling related proteins Src, RhoA, Fyn, Akt1 and phosphatidylinositol 3-kinase did not hinder CVA9 infection in any way (Heikkilä et al. 2010). Instead, macropinocytosis has been recognized to be involved in CVA9 infection (Heikkilä et al. 2010, Huttunen et al. 2014). Later in the infection, CVA9 was found to localize in non-acidifying MVBs approximately 2 h p.i., similarly to E1 (Huttunen et al, 2014). CVA9 was also not associated with early endosome marker EEA1 or late-endosome and lysosome marker Lamp1, further separating the CVA9 from classical lysosomal pathway (Huttunen et al, 2014).

1.5.4 Echovirus 7

E7 was shown to require clathrin for its infection and to co-localize with early endosome marker EEA1 and the late endosome marker LAMP2 during early

infection in polarized human intestinal cells (Caco-2) (Kim and Bergelson, 2012). E7 was also shown not to be dependent on caveolin-1 for its infection. These findings were interesting, as E7 also binds to DAF in its infection but uses completely different endocytic pathway than CVB3 in the same cell line (Kim and Bergelson, 2012). E7 was described to move from early endosomes to late endosomes, but the study was not able to pinpoint any endosomal compartment where viral genome release takes place. This maturation to late endosomes was still necessary for successful infection. As with CVB3, E1 and CVA9, acidification of the virus environment was actually not important for infection, meaning the late endosomes provide some other important signaling factors for E7 genome release (Kim and Bergelson, 2012).

1.6 Aim of the study

Not much is known about the early infection events of E30. Aim of this thesis was to investigate the internalization and localization of E30 inside cells during the first hours of infection. An obvious interest was the receptor usage of E30: due to previous reported association with DAF, and DAF having a strong relation to CAR in the context of enterovirus B species infection, one aim of the study was to study E30 binding to DAF and CAR. Secondly, the kinetics of infection and replication was another interest, whether if follows a typical kinetics of enterovirus B group viruses or if it is more rapid. The third aim was to investigate the nature of the endocytic pathway to cells by perturbing various cellular regulators of clathrin and macropinocytic pathways. As many of the enterovirus B species (apart from EV7 in Caco-2 cells and CVB3 in HeLa cells) are not commonly found to utilize the clathrin and lysosomal pathway, it was hypothesized that E30 would also not use the clathrin pathway. Also, general effects on cellular trafficking were to be studied by monitoring effects on the morophology of endoplasmic reticulum and endosomes. An important technical aim, to facilitate the studies, was to produce and purify E30 in high amounts to be used in infection

studies. As E30 had never been previously purified in Marjomäki group before, the aim was to implement and to optimize the pre-existing protocol used to purify other enterovirus B species for E30.

In this thesis, three batches of E30 were purified using linear sucrose gradient method and purified virus was used for infection studies. Confocal microscopy and co-localization analysis were used to study the E30 association with cellular markers. Time series of infection was performed to measure RNA quantification from confocal images to investigate the rate of E30 replication. Metabolically labeled ^{35S}Met/Cys- E30 was also produced and used to investigate the E30 binding to human DAF and CAR in a non-human cell line.

2 MATERIALS AND METHODS

2.1 Production and purification E30

Human *rhabdomyosarcoma* (RD) cells were cultured in eight 875 cm^2 5-layer flasks using Dulbecco's Modified Eagle Medium (DMEM, Gibco Life Technologies, United Kingdom) supplemented with 10% fetal bovine serum (FBS), 1% GlutaMax (Gibco Life Technologies) and 1% penicillin and streptomycin antibiotics (Gibco Life Technologies, USA). Nearly confluent flasks were infected with E30 (Bastianni sequence) using 5% or 2.5% crude virus stock (CVS, original E30 crude virus stock was kindly provided by M. Lindberg lab, Linnaus University, Sweden) in DMEM supplemented with 1% FBS and 1% Glutamax. Infection was continued in +37°C and 5% CO_2 for 12, 14 or 19 hours.

Collected cell lysate was freeze-thawed three times and broken cell debris was pelleted by centrifuging at 6080 rpm for 30 min at +4°C in Beckman Avanti J-30 I centrifuge with JA-10 rotor. Supernatant was collected and 7% (w/v) PEG-6000 and 2.2% (w/v) NaCl were added to it and mix was stirred at +4°C overnight.

Virus was pelleted by centrifuging at 8000 rpm for 45 min at +4°C in Beckman Avanti J-30 I centrifuge with JA-10 rotor. Supernatant was discarded and pellet was resuspended in 3ml of R-buffer (20mM Tris-HCL pH 7, 200 mM NaCl, 50 mM $MgCl_2$ and 10% glycerol) with help of scraper. Sodium deoxycholate (3 mg/ml) and 100% NP-40 (6 µl/ml) were added and mix was incubated for 30 minutes on ice and mixed every 10 minutes. Solution was centrifuged at 4000g for 15 minutes at +4°C in Thermo Scientific SL 16R centrifuge. Supernatant was collected and added on top of 5-20% linear sucrose gradient made in R-buffer and centrifuged at 35000 rpm for 2 hours at +4°C in Beckman Optima LE-80K Ultracentrifuge with SW-41 rotor. Gradient was collected as 500µl fractions from the top and first 13 fractions were discarded and following 9 fractions were pooled together in Beckmann Optima LE-80K Ultracentrifuges Ti-70 rotor compatible tube. Tube was then filled with 2 mM $MgCl_2$/PBS and virus was concentrated by centrifuging at 35000 rpm for 2h at +4°C. Pellet was resuspended in 200 µl of 2mM $MgCl_2$/PBS and virus was stored in -80°C.

Concentration of the batch was determined using Nanodrop spectrophotometer 1000 (Thermo Scientific) and Beer-Lambert equation, with absorbance (A) at 260 nm and using extinction coefficient of 7.7 (mg/ml)/cm (Basavappa et al. 1998). As Nanodrop spectrophotometer 1000 has a light path of 1 cm and protein/nucleic acid ratio at 260 nm is 0.7, concentration (C) of virus protein can be calculated as:

$$C = \frac{A_{260}}{7.7} \times 0.7 \qquad (1)$$

2.2 End point assay

Infectivity of purified E30 batch was determined with End-Point dilution assay. RD cells were cultured 5000 cells/well on a 96-well plate and grown overnight in DMEM supplemented with 10% FBS, 1% GlutaMax and 1% penicillin and streptomycin antibiotics. Cell monolayers in wells were infected by preparing a dilution series of the virus starting from $x10^{-4}$ down to $x10^{-13}$ in DMEM supplemented with 1% FBS and 1% GlutaMax with eight replicates of every

dilutions. Infection was continued in +37°C and 5% CO_2 incubator and monitored daily until control wells were fully confluent/three days. Infection was then stopped by staining wells with 50 µl of crystal violet stain (8.3 mM crystal violet, 45 mM CaCl2, 10% ethanol, 18.5% formalin, and 35 mM Tris base) for 10 minutes in RT. Plates were washed with water in order to get rid of the excess stain and the 50% tissue culture infective dose (TCID50) was then determined by comparing the number of stained (uninfected) and unstained (infected) wells for eight replicates of each virus concentration. PFU/ml value was then estimated by applying the Poisson distribution and multiplying the TICD50 value by 0.69.

2.3 TEM sample preparation and imaging

Butwar-coated copper grids were glow discharged using EMS/SC7620 Mini Sputter Coating Device according to the manufacturer's instructions. Virus sample was incubated on a 5µl droplet on the grid for 15 seconds and was then blotted away. Viruses were then negatively stained with 1% phosphotungstic acid by adding a 5µl on the grid for 60 seconds and again blotting the excess away. Grids were let to dry overnight and imaged using Jeol JEM-1400HC Transmission Electron Microscope equipped with Olympus SIS QUEMESA bottom-mounted TEM-CCD camera system.

2.4 Production and purification of radioactive ^{35}S-labeled E30

RD cells were cultured in six 75cm^2 flasks in DMEM supplemented with 10% FBS, 1% GlutaMax and 1% penicillin and streptomycin antibiotics until they were nearly confluent. Cells were washed with warm PBS and then incubated in fresh PBS for 15 minutes in +37°C and 5% CO_2 incubator. Cells were infected using 100ul of crude virus stock in Low Methionine/Cysteine MEM (Minimum Essential Medium Eagle with Earle's salts, MP Biomedicals) supplemented with 1%

dialyzed FBS. Medium was replaced after 3h of infection with 1% dialyzed FBS Low Methionine/Cysteine MEM supplemented with 50 µCi/ml of ^{35}S-L-methionine and ^{35}S-L-cysteine mixture (EasyTag Express Protein Labeling Mix [^{35}S], PerkinElmer, Boston). Infection was then continued for 9 more hours.

Collected cell lysate was freeze-thawed three times and broken cell debris was pelleted by centrifuging at 2500 g for 10 minutes at +4°C in Thermo Scientific SL 16R centrifuge. Sodium deoxycholate (3 mg/ml) and 100% NP-40 (20 µl/ml) were added to supernatant and solution was incubated on ice for 30 minutes and mixed every 10 minutes. Solution was then centrifuged at 4000g for 10 minutes at +4°C in Thermo Scientific SL 16R centrifuge. Supernatant was then divided on top of five 40% sucrose/R-buffer cushions laid down in centrifuge tubes. Tubes were filled with 2mM $MgCl_2$/PBS and centrifuged at 35000 rpm for 2.5 hours at +4°C in Beckman Optima LE-80K Ultracentrifuge with SW-41 rotor. After centrifugation, 2mM $MgCl_2$/PBS solution was removed and 500µl fraction was pipetted from the top of cushions and discarded. Next three 500µl fractions were collected from the cushion into Beckmann Optima LE-80K Ultracentrifuges Ti-70 rotor compatible tube. Tube was filled with 2 mM $MgCl_2$/PBS and virus was concentrated by centrifuging at 35000 rpm for 2h at +4°C. Pellet was resuspended in to 1.5 ml of 2 mM $MgCl_2$/PBS and added on top of 5-20% linear sucrose gradient in R-buffer. Sucrose gradient was centrifuged at 35000 rpm for 2 hours at +4°C in Beckman Optima LE-80K Ultracentrifuge with SW-41 rotor. The whole gradient was collected from the top in 500µl fractions and small sample of each fraction was individually mixed with 4ml of Ultima Gold™ MV scintillation cocktail (PerkinElmer). Counts per minute (CPM) value of each fraction was detected using PerkinElmer Liquid Scintillation Analyzer Tri-Carb® 2910 TR. Fractions with the highest CPM values were then pooled together and stored in -80°C.

2.5 Receptor binding assay

Chinese hamster ovaries cells (CHO) were used in receptor binding assay, with one cell line expressing human CAR, one expressing human DAF and one being a wild type control. Cells were cultured in DMEM supplemented with 10% FBS, 1% GlutaMax and 1% penicillin and streptomycin antibiotics. Each cell-line was individually trypzinised and 150 000 cells for each sample was collected. Cells were pelleted by centrifuging at 8000 rpm for 5 minutes at RT in tabletop centrifuge (Eppendorf Centrifuge 5451 D). Supernatant was discarded and pellets were resuspended in 50µl of 2 mM $MgCl_2$/PBS. In the following two replicates of the experiment, this cell pelleting was done with 6000 rpm. Next, 50 000 CPM worth of ^{35}S-labelled E30 (corresponding to MOI 850) was added to each cell suspension and incubated for 60 minutes on ice. Samples were mixed during this incubation by gently tapping the tubes every 20 minutes. Cells were pelleted by centrifuging at 5000 rpm for 5 minutes at +4°C in tabletop centrifuge (Eppendorf Centrifuge 5451 D) and pellets were then resuspended in 100 µl of 2 mM $MgCl_2$/PBS. This pelleting and resuspending was then repeated for second and third time, and on the third time pellet was resuspended in 30ul of µl of 2 mM $MgCl_2$/PBS. Resuspensions were then mixed with 4ml of Ultima Gold™ MV scintillation cocktail (PerkinElmer) and CPM values were detected using PerkinElmer Liquid Scintillation Analyzer Tri-Carb® 2910 TR.

2.6 Infection samples for confocal microscopy

2.6.1 dsRNA & E30 – CD63, CI-MPR & E30 – 1D3 & E30

RD cells were grown overnight on coverslips in DMEM supplemented with 10% FBS, 1% GlutaMax and 1% penicillin and streptomycin antibiotics. Cells were infected using purified virus (2050 PFU/cell) diluted in DMEM supplemented with 1% FBS and 1% GlutaMax. Cold binding was done by incubating cells for 1 hour on ice and then washing cells gently three times with 0,5% BSA/PBS to

remove the excess virus. Fresh 1% DMEM was added and infection was continued in 37°C, 5% CO_2. Infection was stopped at selected time points by removing the medium, quickly washing the cells with PBS and fixing the cells with 4% paraformaldehyde (PFA) by incubating for 30 minutes at RT on a rocker. Coverslips were stored in PBS in +4°C for later use.

2.6.2 Transferrin, EEA1 & E30

RD cells were grown overnight on coverslips in DMEM supplemented with 10% FBS, 1% GlutaMax and 1% penicillin and streptomycin antibiotics. Cells were infected using purified virus (2050 PFU/cell) diluted in DMEM supplemented with 1% FBS and 1% GlutaMax. Cold binding was done by incubating cells for 1 hour on ice and then washing cells gently three times with 0,5% BSA/PBS to remove the excess virus. 50ug/ml of Transferrin- AlexaFluor 488 conjugate (Transferrin from human serum, AlexaFluor 488 conjugate, Invitrogen Molecular Probes) in -DMEM supplemented with 0,2% BSA was added and cells were incubated in 37°C, 5% CO_2. Infection was stopped at 5 min and 30 min timepoints by removing the medium, quickly washing the cells with PBS and fixing the cells with 4% paraformaldehyde (PFA) by incubating for 30 minutes at RT on a rocker. Coverslips were stored in PBS in +4°C for later use.

2.7 Immunolabeling

Infection samples were immmunolabeled against dsRNA, early endosome antigen 1 (EEA1), protein disulfide isomerase or PDI (labelled with 1D3 clone), tetraspanin CD63 (CD63), mannose-6-phosphate receptor (CI-MPR) and E30 capsid protein VP1. Primary antibodies were detected with corresponding secondary antibodies. Specification of used antibodies and dilutions can be found from table 1. Free aldehyde groups were quenched by incubating coverslips in 50mM NH_4Cl for 5 minutes in RT. After that, cells were permeabilized by incubating them in 0,2%

Triton X-100 in PBS for 5 minutes in RT. Coverslips were then washed with PBS quickly. Primary antibodies diluted in 3%BSA/PBS were added as 30ul droplets on top of each coverslip and incubated for 1 hour. Coverslips were washed with PBS 3 x 5 minutes and secondary antibodies diluted in 3% BSA-PBS were added as 30ul droplets on top of each coverslip and incubated for 30 minutes covered from light. PBS washes of 3 x 5 minutes were done again, second wash also containing 300nM DAPI stain (Molecular Probes, Life Technologies, USA). Coverslips were mounted on objective slides with Mowiol supplemented with 25mg/ml of Dabco (Sigma-Aldrich).

Table 1. Antibodies and concentrations used for immunolabeling.

Primary/Secondary	Antibody	Dilution/Final concentration	Origin
Primary	Mouse anti-dsRNA (J2)	125 ng/ml	SCICONS, Hungary
Primary	Rhesus anti-E30	1:100	Kind gift from prof. M. Lindberg, Linnaeus University, Sweden
Primary	Purfied Mouse anti-EEA1	2.5 µg/ml	BD Transduction Laboratories™
Primary	Mouse anti-ID3	1:200	Kind gift from prof. Steve Fuller EMBL, Heidelberg
Primary	Mouse anti-CD63	2.46 µg/ml	Zymed, San-Fransico CA, USA
Primary	Rabbit anti-CI-MPR	1:150	Marjomäki et al. 1990
Secondary	Goat anti-mouse AlexaFluor® 555 and 488	2.5 µg/ml	Molecular Probes Invitrogen, USA
Secondary	Goat anti-rabbit AlexaFluor® 555	2.5 µg/ml	Molecular Probes Invitrogen, USA
Secondary	Goat anti-rhesus IgG(H+L) AlexFluor® 647	2.5 µg/ml	Southern Biotech, USA

2.8 Confocal imaging

Imaging was done using Olympus IX-81 microscope equipped with FV1000 confocal system (405nm diode laser, 488nm argon laser, 543nm and 633nm HeNe laser) and using UPLSAPO 60x oil immersion (Numerical aperture, NA=1.35) and UPLFLN 40x oil immersion (NA=1.30) objectives. Resolution of all acquired images was 640 by 640 pixels.

2.9 dsRNA Quantative analysis

Quantitative analysis of dsRNA signal accumulation during infection was done using BioImage XD software (Kankaanpää et al. 2012). Intensity of the 488nm channels was quantized, with each time point having 11 to 12 images for analysis. Each image contained 5 to 7 cells on average. All images were processed the same way using BioImage XD's batch processing tool. Gaussian smooth was applied with radius factor for x, y, and z set to 1.5 and dimensionality set to 3. Threshold of the 488nm channel was manually set with the help of a negative infection control so that most of the unwanted background noise was removed and signal separated from the background (lower threshold was 60, upper 255). Connected component labeling was set to remove objects with voxel size less than 3. When analyzing segmented objectives, intensity averages and sums, average distances and non-zero voxels were calculated. Object intensity sums of the images were then divided by the cell count (counted manually) of the corresponding images. Each time points' intensity value was averaged and standard errors were calculated.

2.10 Co-localization analysis

Co-localization analysis of confocal images was done using BioImage XD Colocalization tool (Kankaanpää et al. 2012). Lower threshold for E30 channel was set so that no signal was detected in the control samples, while cell marker channels had their full signal coming through. Low thresholds for cell marker channels were then set so that background noise was eliminated. These same settings where then used for all images within one image set. Colocalizing voxels were made visible like this in figures 5 and 6.

3 RESULTS

3.1 Purification and Characterization of E30

Technical aim of this study was to produce and purify E30. As this was never done before, three batches in total (batches #1, #2 and #3) were purified in order to see, whether the used protocol works well for E30. All batches ended up yielding 0.150-309 mg/ml of virus (Table 2). Infectivity of each batch was tested with end point dilution assay, and the results showed good infectivity for all three batches (Table 2). Total amount of infective particles was in the range of 4.30×10^{12} – 2.09×10^{13}.

Table 2. Purified E30 batches.

Batch	E30#1	E30#2	E30#3
Used crude virus stock [%]	5	2.5	2.5
Infection time [h]	14	12	19
$A_{260/280}$	1.56	1.60	1.75
Concentration [mg/ml]	0.309	0.201	0.150
Total virus amount [ug]	61.8	40.2	30.0
Infectivity [PFU/ml]	1.29×10^{12}	2.18×10^{11}	1.29×10^{11}
Total amount of infective particles	2.09×10^{13}	5.42×10^{12}	4.30×10^{12}

Purity of E30 batches was investigated using 12% SDS-PAGE gel (Figure 2, A). E1 sample was included in the gel as a reference sample for viral proteins. Viral proteins VP1, VP2 and VP3 are between 35-25 kDa in size, while VP4 is 7 kDa in size. Every sample showed two bands between 35-25 kDa area, marking VP1 and VP2 or VP3 presence in all samples. VP4 was not detected in any of the samples however. All E30 batches resembled E1 sample greatly and no major impurities were found in any of the batches.

Virus batches were also imaged using transmission electron microscopy (TEM). Negative staining of viruses causes the intact viral particles to show up as white round spots in electron microscope, as the stain encircles the capsid (Figure 2, B). If the particles are not intact, however, stain can enter also inside the capsid and un-intact, empty, particles have thus a dark center, with only capsid outline being white. Batch #1 showed lots of intact particles and only few empty particles (Figure 2, C). Batches #2 and #3 seemed to contain much more empty particles and even some smaller structures that could possibly be unconstructed pentamers (Figure 2, C).

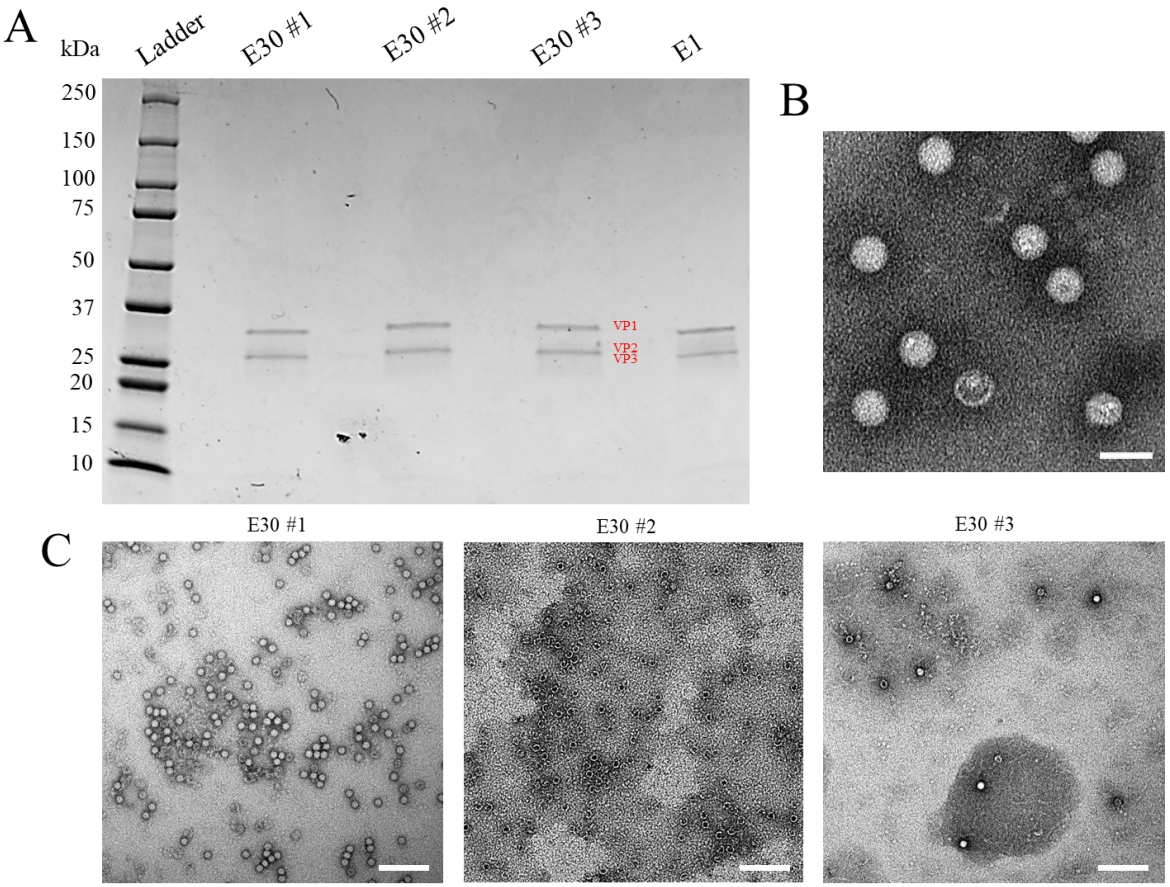

Figure 2. Characterization of E30 batches #1, #2 and #3. **(A)** Purity of the batches was investigated by running the samples in 12% SDS-PAGE gel and staining the gel with Coomassie blue. Previously purified E1 sample was used as a reference. Viral proteins VP1, VP2 and VP3 are between 35-25 kDa in size and they can be detected from the gel. Smaller, approximately 7 kDa sized VP4 cannot be seen on the gel. **(B)** Close up TEM image of E30 particles. Intact particles are colored as white and un-intact empty particles have dark center due to negative stain getting inside the capsid. Scale bar is 40 nm. (C) TEM images of purified batches. E30#1 had many intact particles visible, with some broken particles among them. E30#2 had a higher amount of broken particles visible than E30#1, but still had mostly intact particles. Sample image is from an area with lots of un-intact particles. E30#3 was similar to E30#2, but it had much fewer particles overall. Scale bar in all images is 200 nm.

3.2 Purification of ^{35}S-labelled E30

^{35}S-labelled E30 was purified using 5-20% linear sucrose gradient, which separates virus particles and other components by their mass. Fractions containing the virus particles were determined by measuring the counts per minute (CPM) values of collected 500 µl gradient fractions (Figure 3). Three fractions with highest CPM values and forming the peak of the curve (fractions 17-19) were pooled to be used

in the following experiments. Infectivity of ^{35}S-labelled batch was also tested with end point assay, resulting in infectivity of 3.45 x 10^9 pfu/ml.

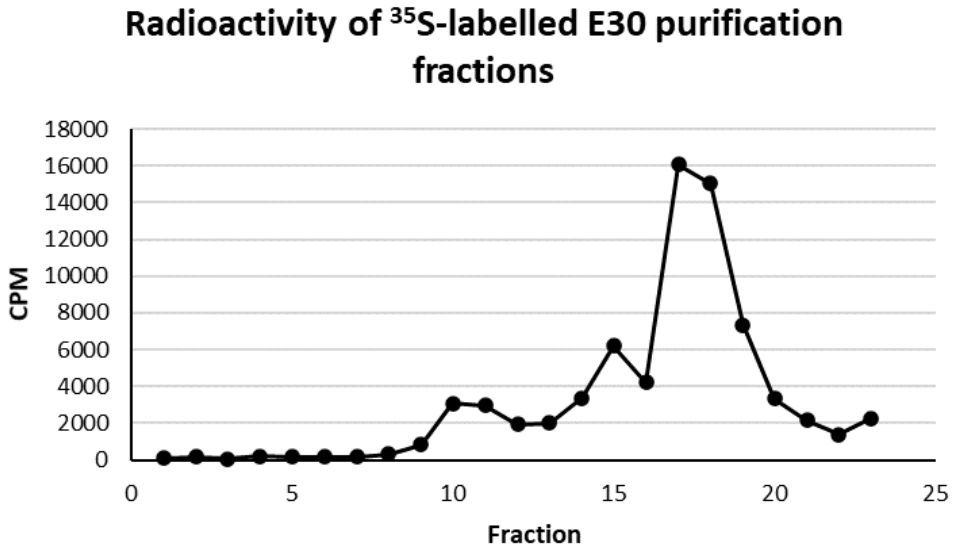

Figure 3. E30 was metabolically labeled with ^{35}S and purified using sucrose gradient. Radioactivity of collected 500 µl sucrose gradient fractions were measured as counts per minute (CPM) to detect, what fractions contained the virus. Fractions 17, 18 and 19 had the highest radioactivity, and were pooled together to be used in the following experiments.

3.3 E30 binds to DAF, but not to CAR

E30 binding to human CAR and human DAF was tested by incubating ^{35}S-labelled E30 with non-infectable CHO cells expressing targets of interest. After binding and washing of the virus, the amount of attached virus was evaluated by measuring samples' CPM value. E30 binding showed strong binding towards DAF, but not CAR (Figure 4). Binding to control cells with no human receptors was minimal and CAR binding showed only very low raise in CPM values. In conclusion, the results showed that E30 bound to the DAF receptor, but not CAR, on the cell surface.

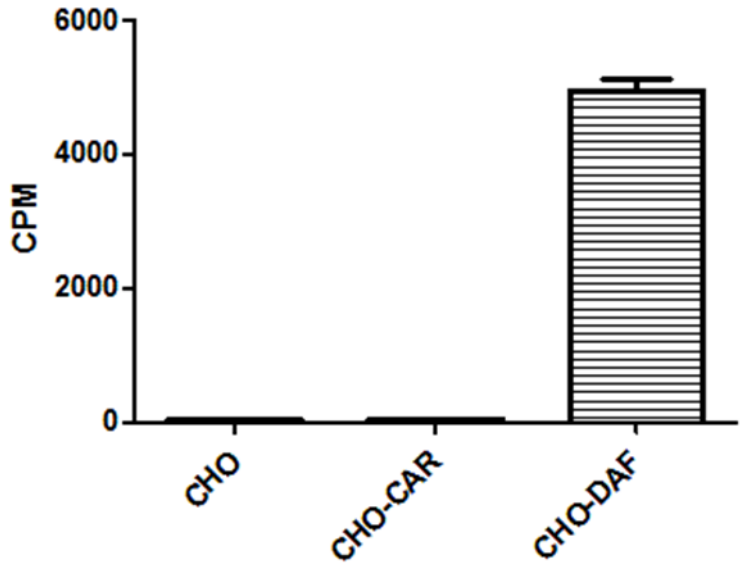

Figure 4. E30 binding to DAF and CAR receptors. Radioactive E30 was bound to wild-type CHO cells or CHO cells expressing human CAR and DAF on ice and excess was washed away. Counts per minute (CPM) of each sample was then measured using liquid scintillation counting. Average values with +/-SEM shown are from three independent experiments, with 3-4 technical replicates of each sample per experiment.

3.5 E30 does not colocalize with clathrin pathway during cell entry, but moves to early endosomes later

Localization of E30 during early infection was investigated with colocalization analysis of confocal microscopy images at 5 min and 30 min p.i. (Figure 5). AlexaFluor 488 conjugated transferrin was used as a marker for clathrin mediated endocytosis pathway and EEA1 antibody was used as a marker for early endosomes. At 5 min p.i., no colocalization between E30 and transferrin was observed, but EEA1 and E30 were found to colocalize in some degree (Figure 5). At 30 min p.i., E30 was found to colocalize with both markers distinctly, most often in the same structures. Colocalization between transferrin and EEA1 can be seen in both timepoints, and also in the control samples.

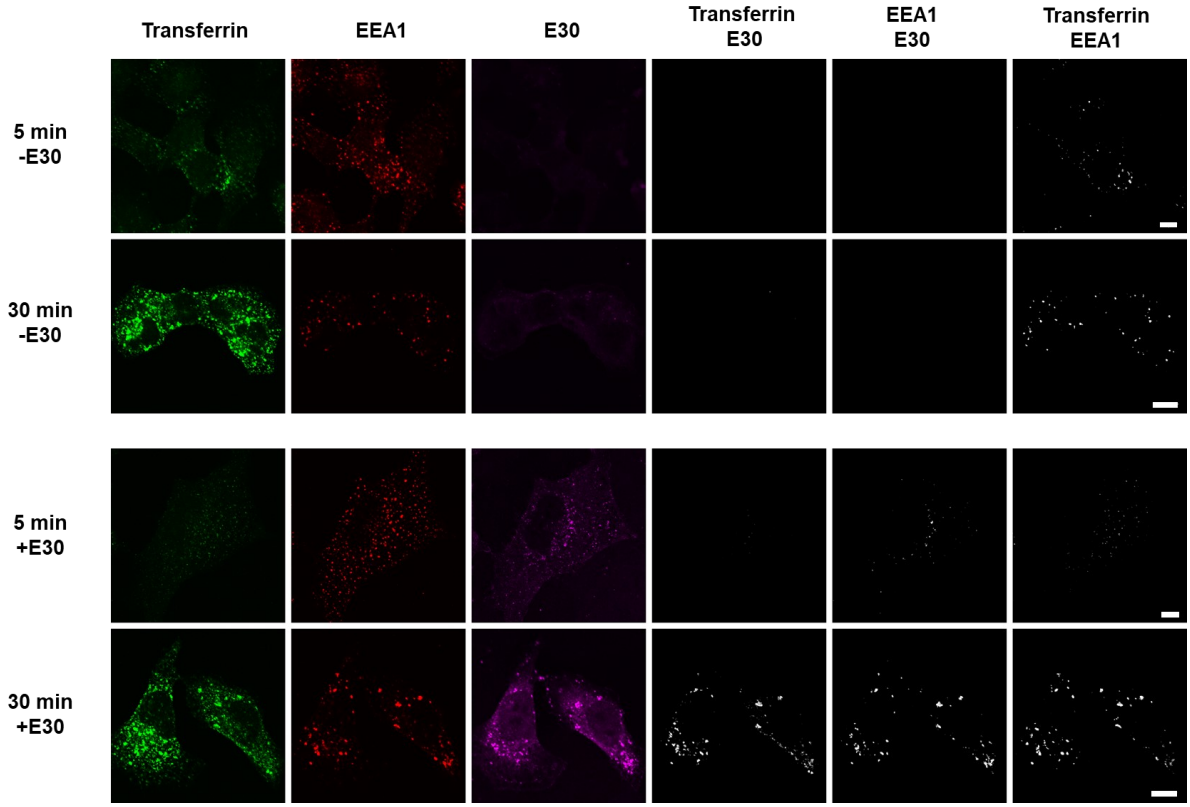

Figure 5. Colocalization of E30 (magenta) between clathrin mediated pathway (transferrin, green) and early endosome structures (EEA1, red) at 5 and 30 min p. i.. White voxels show the colocalizing signal between two markers indicated on top row. Scale bar in all image sets is 10µm.

3.5 E30 colocalizes with late endosome and pre-lysosomal structures

Localization of E30 later in the infection was investigated with colocalization analysis of confocal microscopy images at 1 h and 2 h p.i. (Figure 6). Late endosome-lysosome marker CD63 and late endosome-trans golgi marker CI-MPR were immunolabeled alongside with E30. E30 was found to colocalize with both markers in both 1 h and 2 h time points. Co-localization with CD63 was observed to be stronger than with the CI-MPR. CD63 and CI-MPR were not colocalizing with one another greatly.

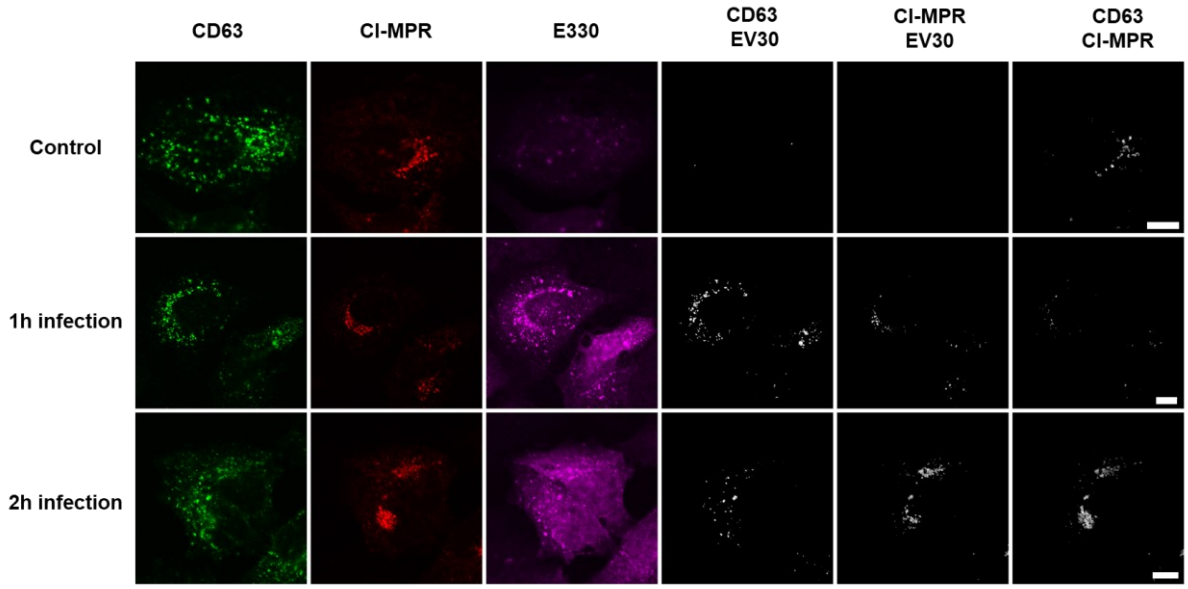

Figure 6. Colocalization of E30 (magenta) with late endosome-lysosome marker CD63 (green) and late endosome-trans-golgi marker CI-MPR (red) at 1 h and 2 h p.i. Mock infection (control) was also visualized. White voxels show the colocalizing signal between two markers indicated on top row. Scale bar in all image sets is 10µm.

3.4 E30 has a rapid infection kinetics

dsRNA intermediates are formed during replication of enterovirus genome, and thus, an antibody against dsRNA can be used to detect the replication of enteroviruses. Signal for dsRNA was quantified from E30 infection series stopped at 1h, 1.5h, 2h, 2.5h, 3, 4h and 5h p.i. time points. The results showed that the dsRNA signal increased and got more intense as the infection went forward (Figure 7, A). Starting from the 4h time point, dsRNA was observed to center near the nucleus of each infected cell. Quantification data obtained from the images showed that the dsRNA signal level started to rise at 2.5h time point, indicating that viral replication started to take off and build up after two hours (Figure 7, B). From this point onward, signal for dsRNA continued to rise from 2.5h to 5h time-point with increasing rate.

A

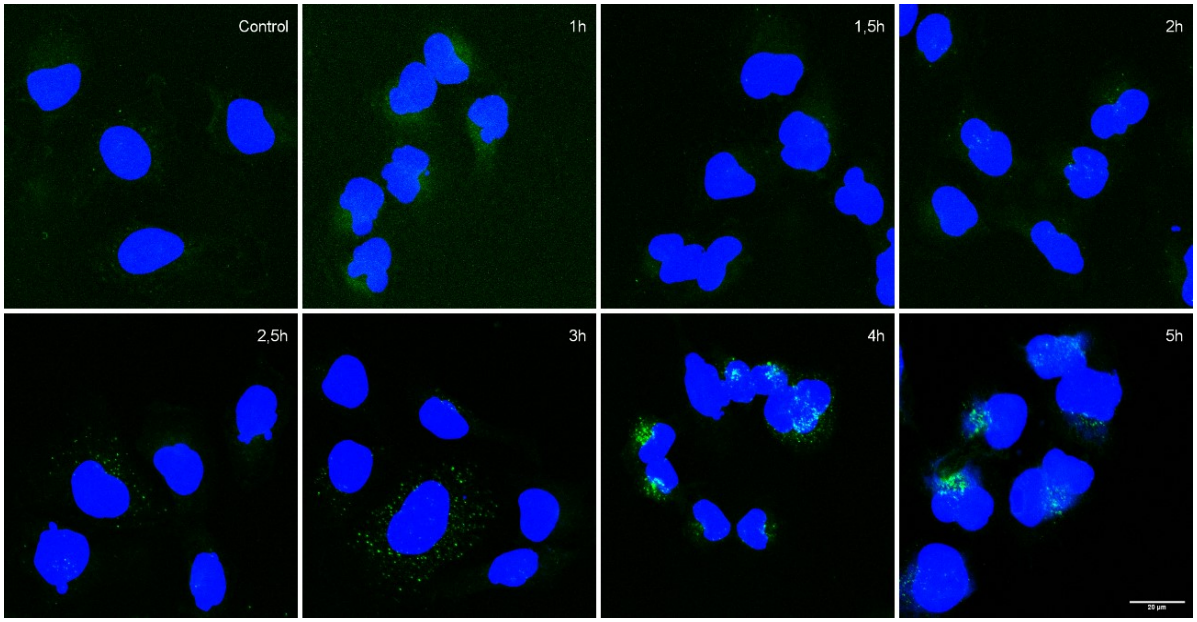

B

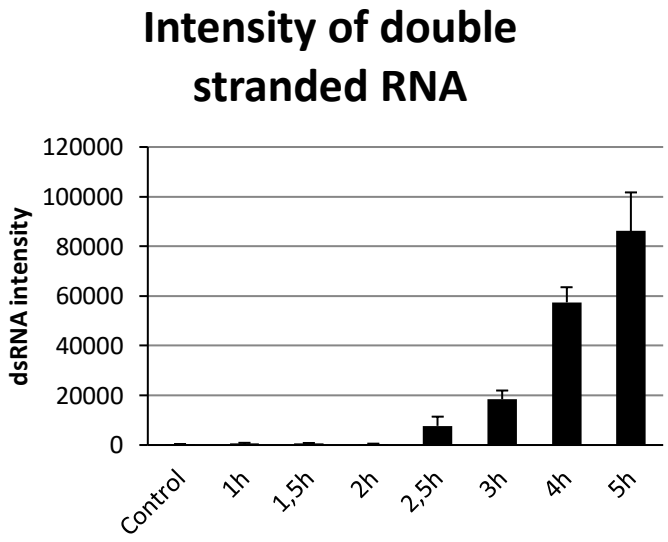

Figure 7. The appearance of E30 dsRNA at 1, 1.5, 2, 2.5, 3, 4 and 5 h p.i. (A) The amount of dsRNA was quantified from sets of confocal microscopy images. Levels of dsRNA (green) were detected to start rising after 2 h p. i.. DAPI (blue) was used to label the nucleus. Scale bar of all images is 20 µm. (B). Average dsRNA intensity and standard deviation of each timepoint was obtained from 10-12 images containing on average 5-7 cells each, with 60–70 cells cells in total for calculations.

3.5 E30 alters the host cell endoplasmic reticulum

1D3 was labeled in order to investigate how E30 infection affects the ER (Figure 8). Very distinct change in ER morphology was seen after a two hour infection, as the ER went from filling the whole cell evenly to shrunken spherical structure to near

vicinity of nucleus. Nucleus itself went through some morphological changes also. E30 particles were scattered throughout the cells, with some being in the near vicinity or under the nucleus.

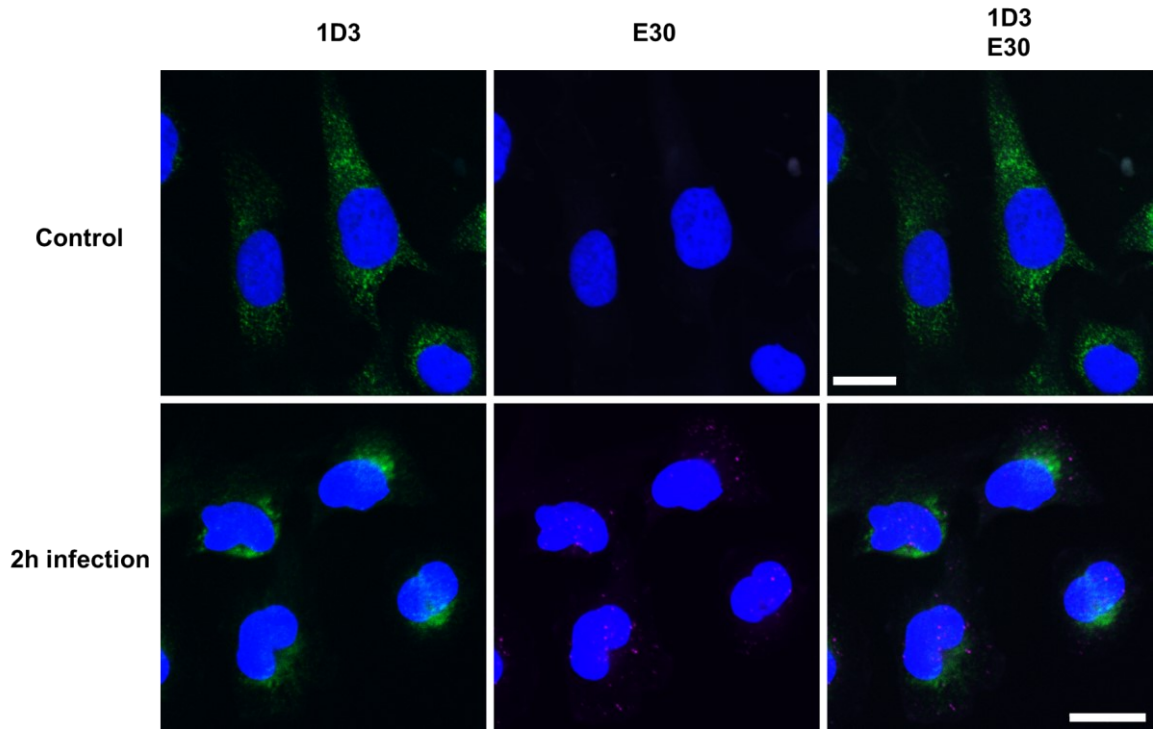

Figure 8. The effect of E30 infection on ER after 2 h. Host cell ER (green) was labelled using 1D3 antibody, DAPI (blue) was used to label the nucleus and E30 was visualized by labeling the capsid protein VP1 (magenta). Scale bar is 20 µm.

4 DISCUSSION

E30 is an enterovirus B species that causes epidemic bursts of viral meningitis around the world. Despite being a major player in the cause of this acute neurological disease, research has started to focus more on E30 biology only in the recent years. Although much is already known about enterovirus B species members and their infection, many pieces of information are still missing. Thus, detailed descriptions of infection mechanisms and host cell interactions of individual species members are still needed. Knowledge already acquired from

other enterovirus B species members has guided research with E30 and similarities and differences in biology between the members are being found.

In this thesis, three batches of E30 were produced and purified to see, how well the used protocol is suiting for E30. The used protocol had previously been used to produce numerous batches of E1, CVB5, and CVA9, with great results. One major difference with E30 production was the use of RD-cells, as normally green monkey kidney (GMK) cells had been cultivated. In the end, RD cells behaved very similarly as GMK cells and their cell cultivation in 5-layer flasks didn't cause any issues. New CVS used for infection was produced from virus material received from M. Lindberg, so that there would be enough material to work with. Titer for CVS was not tested in any way, so the amount of used CVS for infection was varied between produced batches to find a suitable one. Rate of infection and best time for harvest were also unknown, so these were also tested using varying infection times between batches. Rounding and detaching of cells was also monitored during infections. Harvested crude virus lysates were then purified with sucrose gradient and resuspended to same volume.

The E30#1 was produced using 5% crude virus stock and 14h infection time, resulting in highest total virus yield and titer of all three batches (Table 1). $A_{260/280}$ ratio of 1.7 is considered as optimal ratio for enterovirus nucleic acid/protein relation and E30#1 showed slightly elevated protein concentrations. This could be due to collecting the sucrose gradient fractions rather broadly, which probably resulted in the collection of also empty capsids found typically on the top parts of the gradient. No unknown proteins were found from SDS-PAGE assay when compared to E1 batch, supporting the theory that the elevated protein amounts were viral and not host cell origin. Furthermore, empty particles were also present in electron microscopy samples (Figure 2, C). According to the end point assay, the infectivity of E30#1 was great, however, and was on similar levels as with previously produced E1 and CVA9. Lower total virus amounts of E30#2 and E30#3 were most likely due to less CVS being used, as less cells were effectively

infected. The fact that in batch E30#1 only 7 out of 8 5-layer flasks were actually infected and collected supports this, as the batch resulted in higher yield even with lower cell amount. In batch #2, harvest after 12 h was tested, as most of the infected cells started to detach already at this point also during E30#1 production. Harvesting as late as after 19 h was also tested in the E30#3, as it is closer to time point when E1 for example is usually harvested. Ideal harvest time for the used CVS is clearly in between 12-14 h, as extended infection resulted in lower yield. Purity of E30#2 and E30#3 were slightly better than E30#1, but they also had significantly more empty particles visible in TEM images. The amount of intact particles in both batches was still considered good and the batches also showed high infectivity according to PFU/ml values. Although all batches were considered to be well suited for use in the subsequent experiments, all the following studies in this master's thesis were done using the E30#1. In order to optimize virus production in the future, titer of used CSV should be measured and proper MOI and infection time should be determined and used for optimal and consistent production.

Radioactive E30 was produced to be used in cell receptor binding assay. Same concerns were again present for production and purification, as neither RD-cells nor E30 were previously used with this protocol. GMK cells had been previously used for the production of radioactive E1 and CVB3 with great results. Unfortunately, 15 minutes incubation in PBS before infection caused some of the RD-cells to detach and wash away when changing the PBS to medium. This lower cell amount most likely affected virus yield negatively, which was seen already when measuring CPM values for collected sucrose gradient fractions. Thus, final concentration step that is usually included in the protocol was not performed, as there was a concern that low virus amount would not form a good and visible pellet during the ultracentifugation and that final product would be lost. Final ^{35}S-labelled E30 batch had rather low CPM value and relatively large volumes were

required for binding assays. Infectivity of the batch was also very low (3.45×10^9 PFU/ml) due to low virus concentration.

Using the ^{35}S-labelled E30, we showed that E30 binds to DAF with great affinity, but does not bind to CAR. This clear binding to DAF is well in line with previously published studies (Bergelson et al., 1994, Zhao et al. 2019). E30 showing no binding to CAR suggest that it is not using similar DAF-CAR interaction based entry pathway as CVB serotypes (Coyne and Bergelson, 2006). Indeed, after experimental part of this thesis was done, new data has been published which strongly suggests that neonatal Fc-receptor (FcRn) works as the primary receptor for many echoviruses, including E30, E7 and also CVA9 (Morosky et al. 2019, Zhao et al. 2019). FcRn is a MHC class I type molecule expressed in numerous organs throughout the human body and it has important roles in regulation of blood albumin and IgG homeostasis and immune response (Baker et al. 2009). Morosky et al. (2019) not only showed that silencing of Fc-receptor expression and blocking of receptor binding prevents infection of various echoviruses, but also that introducing a human Fc-receptor to normally non-permissive human and mouse cells renders them sensitive for infection. Zhao et al. (2019) described the neonatal Fc-receptor as main uncoating receptor for echoviruses and proposed that DAF works as a similar attachment and transfer receptor between echoviruses and FcRn, as it does between CVB3 and CAR. Similarly as with CVB3, echovirus binding to DAF does not show to cause the formation of A-particle (Zhao et al. 2019). It is still unclear, however, whether DAF transfers the virus to Fc-receptor on the cell membrane and Fc-receptor binding causes the internalization or whether DAF binding itself causes the internalization and the virus binds to the Fc-receptor in the endosomes, causing the formation of the A-particle in there (Zhao et al. 2019). Data is showing more towards the latter, as it was shown that DAF localizes mainly on the cell surface and the Fc-receptor more in the cytosol, possibly inside endosomes (Zhao et al. 2019). The role of the FcRn in E30 infection was also later confirmed in our following experiments, where a siRNA knockout

of the FcRn in the human lung carcinoma cells (A549) prevented the infection completely (Vandesande et al. 2020). As an even more interesting note, our following studies also showed that siRNA knockout of DAF did not prevent the E30 infection at all, although the E30 has been shown to have great binding affinity towards DAF by us and others (Vandesande et al. 2020). It is very possible however, that the DAF's role as an infection promoting co-receptor for FcRn is actualized only in the polarized epithelial cells, as it is in the case of CVB3 and CAR.

E30 was shown to colocalize with early endosome marker EEA1 during early infection. This was an interesting finding, as many of the enterovirus B members have not been found to localize in the early endosomes (Marjomäki et al. 2015). However, E7 has been observed to localize in the early endosomes and it is also logical, as it was also shown to use the clathrin mediated endocytic pathway (Kim and Bergelson, 2012). Clathrin mediated endosomes being sorted into the early endosomes over time can also be observed from our data, as transferrin colocalization with EEA1 increased from 5 min time point to 30 min time greatly (Figure 5). Given that both E30 and E7 have been shown to use DAF and FcRn for their infection and to localize in early endosomes after internalization, one could easily argue that E30 would also use the clathrin mediated endocytosis pathway for its entry. Our data suggest otherwise, as no colozalization between transferrin and E30 was observed after 5 min p.i. (Figure 5). Colocalization increased significantly after 30 min p.i., but this happens due to transferrin and E30 both being sorted into early endosomes. This suggested that E30 was not budding from clathrin coated pits, but rather from the raft domains on the plasma membrane. Raft usage is also supported by the finding in our following studies that filipin perturbs E30 entry (Vandesande et al. 2020). Role of clathrin mediated endocytosis in E30 entry should still be confirmed in the future using siRNA interference or other knock-out methods targeting clathrin and other key players involved, such

as dynamin-2 and Eps15. In addition, quantification of colocalization data should also be performed.

As a natural continuum of being localized in early endosomes, E30 was also shown to colocalize with late endosome-lysosomal marker CD63 and late endosome-trans-golgi marker CI-MPR. In context of classical lysosomal pathway, early endosomes maturate, or their cargo is being transferred, into late endosomes and further from there to lysosomes. Already after 1 h p.i., E30 was colocalizing with both of the markers and continued to do so also at 2 h p.i. (Figure 6). Observed co-localization is clearly stronger with CD63, however, and markers don't show to co-localize with one another that much. Yet again, these results regarding the E30 need to be verified with varying methodology, such as siRNA study preventing E30 entry to the late endosomes and impact of that to overall infection. More precise time series with quantified co-localization data starting already from earlier time points would also provide a greatly accurate time table for E30 infection.

This E30 localizing in late endosomes again resembles the E7 infection, as E7 was also observed to colocalize with late endosome and lysosome marker Lamp2 (Kim and Bergelson, 2012). After the experimental part of this thesis, the question remained how important this endosomal maturation and lowering of environment pH is for E30? It is was held as very likely that the E30 does not require the acidification of the endosomes for its infection, as it has been the case with the great majority of the studied enterovirus B members and E7 as well. This hypothesis was indeed later confirmed to be true in our following experiments, as treating cells with lysosomal acidification preventing drug Bafilomycin A1 (Mauvezin et Neufeld, 2015) did not show to have any effect on E30 infection (Vandesande et al. 2020). It is likely that the viral genome egresses already before the lysosomal stage, and thus, acidification does not play a role in the genome release, although the viral capsid eventually ends up in the lysosomal pathway.

Now the great question lies, what factor(s) in the endosomal pathway is necessary for E30 and E7 genome egress?

E30 was shown to have quite rapid timetable for its infection, as presence of dsRNA was detected already after at 2.5 h p.i. (Figure 7). Levels of dsRNA started rising rapidly after 3 h p.i. and cells started to round up and detach at 6 h and 7 h p.i. (data not shown). This fast infection and replication was noticed also during mass production of the virus, as the majority of cells in the 5-layer flasks started to round up and detach already at 12 h p.i., whereas with the E1 and CVA9 this stage has been typically achieved at 18–22 h p.i.. Varying amount of used crude virus lysate might have affected this rate of infection however. Uncoating of CVA9 has been shown to happen at 2 h p.i., while dsRNA was detected starting at 3 h p.i. (Huttunen et al. 2014). However, CVA9 dsRNA might have been present already before, as no time point between 2 h and 3 h was tested. Levels of dsRNA during CVB3 infection have been reported to increase only after 3 h timepoint with a qPCR assay (Limpens et al. 2011). A study with single assay between different species would be required for a comparison of early infection rate reliably.

E30 was also shown to cause alterations in the morphology of the ER. ER was visualized by labelling protein disulfide isomerase, an enzyme found inside ER, with 1D3 clone antibody (Vaux et al. 1990). Control cells showed an even distribution of the ER throughout the cell, while E30 caused it to shrunken into near vicinity of cell nucleus at 2 h p.i.. (Figure 8). This rearrangement of the ER is most likely part of the formation of the replication organelles enteroviruses have been shown to form (van der Schaar et al. 2016). Interestingly enough, ROs have been described to appear only later during infection (4 h p.i.) and first being single membraned but later turning into double-membraned multilamellar tubular like structures, that most likely originate from Golgi apparatus (Limpens et al. 2011, Belov et al. 2012). These changes are thought to be caused by activity of viral proteins 2B, 2C and 3A accumulating during infection (Cho et al. 1994, Barco et Carrasco 1995, Suhy et al. 2000). In the case of EV71, ER stress was also reported to

be caused by viral replication rather than virus entry (Jheng et al. 2010). In addition, the rearrangement of vimentin filaments into a cage-like structure near the nucleus has been shown to happen during E1, CVB1 and CVA9 infections (Turkki et al. 2020). The vimentin cage surrounded the dsRNA and also resulted in the redistribution of ER close to the nucleus, suggesting that the replication was taking place on ER membranes inside the vimentin cage. However, this was also happening more after 4 h p.i. (Turkki et al. 2020). The concentration of dsRNA near the nucleus can also be seen in the dsRNA quantification assay with E30, starting at 4 h time point (Figure 7, A). Given that E30 seems to have rather rapid infection altogether, the observed early modifications on ER could be part of the preparation for the RNA replication observed starting already at 2.5 h p.i. (Figure 7, B). Early effect of E30 on ER seems still somewhat extraordinary and should be studied further.

In conclusion, three normal batches and one radioactive batch of E30 were produced and purified successfully. Binding assay done using radioactive E30 clearly showed that E30 binds to DAF, but not to CAR. Infection studies with purified E30 in RD-cells showed that E30 does not seem to use clathrin mediated endocytic pathway for its internalization, but it still moves to early endosome structures during the first 30 minutes of infection. At 1 and 2 h p.i., E30 can be found from late endosome structures. First signs of RNA replication can be seen at 2.5 h p.i., after which replication continues and increases exponentially. E30 also alters the host cell ER membranes already at 2 h p.i. These results combined with the new findings of the FC-receptor role on the echovirus infection make the E30 infection resemble the behavior of E7 the most, with possible differences regarding cell internalization and infection rate. As there are still many echoviruses not yet studied further, it will be interesting to learn in the future whether all of them have similar behavior and infection or if the E30 has some unique properties that differs it from the rest, making it more susceptible for causing the aseptic meningitis.

ACKNOWLEDGEMENTS

I would like to thank my supervisors Varpu Marjomäki and Michael Lindberg for this thesis opportunity and for their patient guidance helping me to finish my work. I would also like to thank the whole Marjomäki group and Helena Vandesande for their help and support. Special thanks goes to Mira Laajala for helping and brainstorming ideas during the lab work and for valuable feedback during writing of the thesis.

REFERENCES

Asher D.R., Cerny A.M., Weiler S.R., Horner J.W., Keeler M.L., Neptune M.A., Jones S.N., Bronson R.T., Depinho R.A. & Finberg R.W. 2005. Coxsackievirus and adenovirus receptor is essential for cardiomyocyte development. *Genesis* 42: 77-85.

Baker K., Qiao S., Kuo T., Kobayashi K., Yoshida M., Lencer W.I. & Blumberg R.S. 2009. Immune and non-immune functions of the (not so) neonatal Fc receptor, FcRn. *Semin Immunopathol* 31: 223-236.

Bandyopadhyay A.S., Garon J., Seib K. & Orenstein W.A. 2015. Polio vaccination: past, present and future. *Future Microbiol* 10: 791-808.

Barco A. & Carrasco L. 1995. A human virus protein, poliovirus protein 2BC, induces membrane proliferation and blocks the exocytic pathway in the yeast Saccharomyces cerevisiae. *EMBO J* 14: 3349-3364.

Basavappa R., Gómez-Yafal A. & Hogle J.M. 1998. The Poliovirus Empty Capsid Specifically Recognizes the Poliovirus Receptor and Undergoes Some, but Not All, of the Transitions Associated with Cell Entry. *J Virol* 72: 7551-7556.

Begier E.M., Oberste M.S., Landry M.L., Brennan T., Mlynarski D., Mshar P.A., Frenette K., Rabatsky-Ehr T., Purviance K., Nepaul A., Nix W.A., Pallansch M.A., Ferguson D., Cartter M.L. & Hadler J.L. 2008. An outbreak of concurrent echovirus 30 and coxsackievirus A1 infections associated with sea swimming among a group of travelers to Mexico. *Clin Infect Dis* 47: 616-623.

Belov G.A., Nair V., Hansen B.T., Hoyt F.H., Fischer E.R. & Ehrenfeld E. 2012. Complex dynamic development of poliovirus membranous replication complexes. *J Virol* 86: 302-312.

Bergelson J.M., Mohanty J.G., Crowell R.L., St John N.F., Lublin D.M. & Finberg R.W. 1995. Coxsackievirus B3 adapted to growth in RD cells binds to decay-accelerating factor (CD55). *J Virol* 69: 1903-1906.

Bergelson J.M., Chan M., Solomon K.R., St John N.F., Lin H. & Finberg R.W. 1994. Decay-accelerating factor (CD55), a glycosylphosphatidylinositol-anchored complement regulatory protein, is a receptor for several echoviruses. *Proc Natl Acad Sci U S A* 91: 6245-6248.

Bergelson J.M., Shepley M.P., Chan B.M., Hemler M.E. & Finberg R.W. 1992. Identification of the integrin VLA-2 as a receptor for echovirus 1. *Science* 255: 1718-1720.

Bergelson J.M., Cunningham J.A., Droguett G., Kurt-Jones E.A., Krithivas A., Hong J.S., Horwitz M.S., Crowell R.L. & Finberg R.W. 1997. Isolation of a common receptor for Coxsackie B viruses and adenoviruses 2 and 5. *Science* 275: 1320-1323.

Buchta D., Füzik T., Hrebík D., Levdansky Y., Sukeník L., Mukhamedova L., Moravcová J., Vácha R. & Plevka P. 2019. Enterovirus particles expel capsid pentamers to enable genome release. *Nat Commun* 10.

Chen Y., Du W., Hagemeijer M.C., Takvorian P.M., Pau C., Cali A., Brantner C.A., Stempinski E.S., Connelly P.S., Ma H., Jiang P., Wimmer E., Altan-Bonnet G. & Altan-Bonnet N. 2015. Phosphatidylserine vesicles enable efficient en bloc transmission of enteroviruses. *Cell* 160: 619-630.

Cho M.W., Teterina N., Egger D., Bienz K. & Ehrenfeld E. 1994. Membrane rearrangement and vesicle induction by recombinant poliovirus 2C and 2BC in human cells. *Virology* 202: 129-145.

Choi Y.J., Park K.S., Baek K.A., Jung E.H., Nam H.S., Kim Y.B. & Park J.S. 2010. Molecular characterization of echovirus 30-associated outbreak of aseptic meningitis in Korea in 2008. *J Microbiol Biotechnol* 20: 643-649.

Chung S., Kim J., Kim I., Park S., Paek K. & Nam J. 2005. Internalization and trafficking mechanisms of coxsackievirus B3 in HeLa cells. *Virology* 333: 31-40.

Cohen C.J., Shieh J.T.C., Pickles R.J., Okegawa T., Hsieh J. & Bergelson J.M. 2001. The coxsackievirus and adenovirus receptor is a transmembrane component of the tight junction. *Proc Natl Acad Sci U S A* 98: 15191-15196.

Coyne C.B. & Bergelson J.M. 2006. Virus-induced Abl and Fyn kinase signals permit coxsackievirus entry through epithelial tight junctions. *Cell* 124: 119-131.

Doherty G.J. & McMahon H.T. 2009. Mechanisms of endocytosis. *Annu Rev Biochem* 78: 857-902.

Duncan I.B. 1968. A comparative study of 63 strains of ECHO virus type 30. *Arch Gesamte Virusforsch* 25: 93-104.

Faustini A., Fano V., Muscillo M., Zaniratti S., La Rosa G., Tribuzi L. & Perucci C.A. 2006. An outbreak of aseptic meningitis due to echovirus 30 associated with attending school and swimming in pools. *Int J Infect Dis* 10: 291-297.

Feng Z., Hensley L., McKnight K.L., Hu F., Madden V., Ping L., Jeong S., Walker C., Lanford R.E. & Lemon S.M. 2013. A pathogenic picornavirus acquires an envelope by hijacking cellular membranes. *Nature* 496: 367-371.

Fricks C.E. & Hogle J.M. 1990. Cell-induced conformational change in poliovirus: externalization of the amino terminus of VP1 is responsible for liposome binding. *J Virol* 64: 1934-1945.

Fields B.N., Knipe D.M. & Howley P.M. 2013. *Fields virology*. Wolters Kluwer Health/Lippincott Williams & Wilkins, Philadelphia.

Friedrichson T. & Kurzchalia T.V. 1998. Microdomains of GPI-anchored proteins in living cells revealed by crosslinking. *Nature* 394: 802-805.

Goodfellow I.G., Evans D.J., Blom A.M., Kerrigan D., Miners J.S., Morgan B.P. & Spiller O.B. 2005. Inhibition of Coxsackie B Virus Infection by Soluble Forms of Its Receptors: Binding Affinities, Altered Particle Formation, and Competition with Cellular Receptors. *J Virol* 79: 12016-12024.

Heikkilä O., Susi P., Tevaluoto T., Härmä H., Marjomäki V., Hyypiä T. & Kiljunen S. 2010. Internalization of coxsackievirus A9 is mediated by {beta}2-microglobulin, dynamin, and Arf6 but not by caveolin-1 or clathrin. *J Virol* 84: 3666-3681.

Hidaka C., Milano E., Leopold P.L., Bergelson J.M., Hackett N.R., Finberg R.W., Wickham T.J., Kovesdi I., Roelvink P. & Crystal R.G. 1999. CAR-dependent and CAR-independent pathways of adenovirus vector-mediated gene transfer and expression in human fibroblasts. *J Clin Invest* 103: 579-587.

Holmes C.W., Koo S.S.F., Osman H., Wilson S., Xerry J., Gallimore C.I., Allen D.J. & Tang J.W. 2016. Predominance of enterovirus B and echovirus 30 as cause of viral meningitis in a UK population. *J Clin Virol* 81: 90-93.

Huttunen M., Waris M., Kajander R., Hyypiä T. & Marjomäki V. 2014. Coxsackievirus A9 infects cells via nonacidic multivesicular bodies. *J Virol* 88: 5138-5151.

Jheng J., Lau K.S., Tang W., Wu M. & Horng J. 2010. Endoplasmic reticulum stress is induced and modulated by enterovirus 71. *Cell Microbiol* 12: 796-813.

Kankaanpää P., Paavolainen L., Tiitta S., Karjalainen M., Päivärinne J., Nieminen J., Marjomäki V., Heino J. & White D.J. 2012. BioImageXD: an open, general-purpose and high-throughput image-processing platform. *Nat Methods* 9: 683-689.

Karjalainen M., Rintanen N., Lehkonen M., Kallio K., Mäki A., Hellström K., Siljamäki V., Upla P. & Marjomäki V. 2011. Echovirus 1 infection depends on biogenesis of novel multivesicular bodies. *Cell Microbiol* 13: 1975-1995.

Karjalainen M., Kakkonen E., Upla P., Paloranta H., Kankaanpää P., Liberali P., Renkema G.H., Hyypiä T., Heino J. & Marjomäki V. 2008. A Raft-derived, Pak1-regulated Entry Participates in α2β1 Integrin-dependent Sorting to Caveosomes. *Mol Biol Cell* 19: 2857-2869.

Kim C. & Bergelson J.M. 2012. Echovirus 7 entry into polarized intestinal epithelial cells requires clathrin and Rab7. *mBio* 3.

Künkel U. & Schreier E. 2000. Genetic variability within the VP1 coding region of echovirus type 30 isolates. *Arch Virol* 145: 1455-1464.

Laitinen O.H., Svedin E., Kapell S., Nurminen A., Hytönen V.P. & Flodström-Tullberg M. 2016. Enteroviral proteases: structure, host interactions and pathogenicity. *Rev Med Virol* 26: 251-267.

Limpens, Ronald W. A. L., van der Schaar, Hilde M., Kumar D., Koster A.J., Snijder E.J., van Kuppeveld, Frank J. M. & Bárcena M. 2011. The transformation of enterovirus replication structures: a three-dimensional study of single- and double-membrane compartments. *mBio* 2.

Marjomäki V.S., Huovila A.P., Surkka M.A., Jokinen I. & Salminen A. 1990. Lysosomal trafficking in rat cardiac myocytes. *J Histochem Cytochem* 38: 1155-1164.

Marjomäki V., Turkki P. & Huttunen M. 2015. Infectious Entry Pathway of Enterovirus B Species. *Viruses* 7: 6387-6399.

Martino T.A., Petric M., Weingartl H., Bergelson J.M., Opavsky M.A., Richardson C.D., Modlin J.F., Finberg R.W., Kain K.C., Willis N., Gauntt C.J. & Liu P.P. 2000. The coxsackie-adenovirus receptor (CAR) is used by reference strains and clinical isolates representing all six serotypes of coxsackievirus group B and by swine vesicular disease virus. *Virology* 271: 99-108.

Mauvezin C. & Neufeld T.P. 2015. Bafilomycin A1 disrupts autophagic flux by inhibiting both V-ATPase-dependent acidification and Ca-P60A/SERCA-dependent autophagosome-lysosome fusion. *Autophagy* 11: 1437-1438.

Mercer J., Schelhaas M. & Helenius A. 2010. Virus entry by endocytosis. *Annu Rev Biochem* 79: 803-833.

Morosky S., Wells A.I., Lemon K., Evans A.S., Schamus S., Bakkenist C.J. & Coyne C.B. 2019. The neonatal Fc receptor is a pan-echovirus receptor. *Proc Natl Acad Sci U S A* 116: 3758-3763.

Nikonov O.S., Chernykh E.S., Garber M.B. & Nikonova E.Y. 2017. Enteroviruses: Classification, Diseases They Cause, and Approaches to Development of Antiviral Drugs. *Biochemistry Mosc* 82: 1615-1631.

Organtini L.J., Makhov A.M., Conway J.F., Hafenstein S. & Carson S.D. 2014. Kinetic and Structural Analysis of Coxsackievirus B3 Receptor Interactions and Formation of the A-Particle. *J Virol* 88: 5755-5765.

Palacios G., Casas I., Cisterna D., Trallero G., Tenorio A. & Freire C. 2002. Molecular Epidemiology of Echovirus 30: Temporal Circulation and Prevalence of Single Lineages. *J Virol* 76: 4940-4949.

Panjwani A., Strauss M., Gold S., Wenham H., Jackson T., Chou J.J., Rowlands D.J., Stonehouse N.J., Hogle J.M. & Tuthill T.J. 2014. Capsid protein VP4 of human rhinovirus induces membrane permeability by the formation of a size-selective multimeric pore. *PLoS Pathog* 10: e1004294.

Patel K.P., Coyne C.B. & Bergelson J.M. 2009. Dynamin- and lipid raft-dependent entry of decay-accelerating factor (DAF)-binding and non-DAF-binding coxsackieviruses into nonpolarized cells. *J Virol* 83: 11064-11077.

Pickl-Herk A., Luque D., Vives-Adrián L., Querol-Audí J., Garriga D., Trus B.L., Verdaguer N., Blaas D. & Castón J.R. 2013. Uncoating of common cold virus is preceded by RNA switching as determined by X-ray and cryo-EM analyses of the subviral A-particle. *Proc Natl Acad Sci U S A* 110: 20063-20068.

Pietiäinen V., Marjomäki V., Upla P., Pelkmans L., Helenius A. & Hyypiä T. 2004. Echovirus 1 Endocytosis into Caveosomes Requires Lipid Rafts, Dynamin II, and Signaling Events. *Mol Biol Cell* 15: 4911-4925.

Pinto Junior V.L., Rebelo M.C., Costa E.V.d., Silva E.E.d. & Bóia M.N. 2009. Description of a widespread outbreak of aseptic meningitis due to echovirus 30 in Rio de Janeiro state, Brazil. *Braz J Infect Dis* 13: 367-370.

Powell R.M., Schmitt V., Ward T., Goodfellow I., Evans D.J. & Almond J.W. 1998. Characterization of echoviruses that bind decay accelerating factor (CD55): evidence that some haemagglutinating strains use more than one cellular receptor. *J Gen Virol* 79 (Pt 7): 1707-1713.

Ren J., Wang X., Hu Z., Gao Q., Sun Y., Li X., Porta C., Walter T.S., Gilbert R.J., Zhao Y., Axford D., Williams M., McAuley K., Rowlands D.J., Yin W., Wang J., Stuart D.I., Rao Z. & Fry E.E. 2013. Picornavirus uncoating intermediate captured in atomic detail. *Nat Commun* 4: 1929.

Rintanen N., Karjalainen M., Alanko J., Paavolainen L., Mäki A., Nissinen L., Lehkonen M., Kallio K., Cheng R.H., Upla P., Ivaska J. & Marjomäki V. 2012. Calpains promote α2β1 integrin turnover in nonrecycling integrin pathway. *Mol Biol Cell* 23: 448-463.

Roelvink P.W., Lizonova A., Lee J.G.M., Li Y., Bergelson J.M., Finberg R.W., Brough D.E., Kovesdi I. & Wickham T.J. 1998. The Coxsackievirus-Adenovirus Receptor Protein Can Function as a Cellular Attachment Protein for Adenovirus Serotypes from Subgroups A, C, D, E, and F. *J Virol* 72: 7909-7915.

Roivainen M., Alfthan G., Jousilahti P., Kimpimäki M., Hovi T. & Tuomilehto J. 1998. Enterovirus infections as a possible risk factor for myocardial infarction. *Circulation* 98: 2534-2537.

Savolainen C., Hovi T. & Mulders M.N. 2001. Molecular epidemiology of echovirus 30 in Europe: succession of dominant sublineages within a single major genotype. *Arch Virol* 146: 521-537.

Sobo K., Rubbia-Brandt L., Brown T.D.K., Stuart A.D. & McKee T.A. 2011. Decay-accelerating factor binding determines the entry route of echovirus 11 in polarized epithelial cells. *J Virol* 85: 12376-12386.

Soonsawad P., Paavolainen L., Upla P., Weerachatyanukul W., Rintanen N., Espinoza J., McNerney G., Marjomäki V. & Cheng R.H. 2014. Permeability changes of integrin-containing multivesicular structures triggered by picornavirus entry. *PLoS ONE* 9: e108948.

Suhy D.A., Giddings T.H. & Kirkegaard K. 2000. Remodeling the endoplasmic reticulum by poliovirus infection and by individual viral proteins: an autophagy-like origin for virus-induced vesicles. *J Virol* 74: 8953-8965.

Too I.H.K., Yeo H., Sessions O.M., Yan B., Libau E.A., Howe J.L.C., Lim Z.Q., Suku-Maran S., Ong W., Chua K.B., Wong B.S., Chow V.T.K. & Alonso S. 2016. Enterovirus 71 infection of motor neuron-like NSC-34 cells undergoes a non-lytic exit pathway. *Sci Rep* 6: 36983.

Turkki P., Laajala M., Flodström-Tullberg M. & Marjomäki V. 2020. Human Enterovirus Group B Viruses Rely on Vimentin Dynamics for Efficient Processing of Viral Nonstructural Proteins. *J Virol* 94.

Tuthill T.J., Groppelli E., Hogle J.M. & Rowlands D.J. 2010. Picornaviruses. *Curr Top Microbiol Immunol* 343: 43-89.

van der Schaar, Hilde M., Dorobantu C.M., Albulescu L., Strating, Jeroen R. P. M. & van Kuppeveld, Frank J. M. 2016. Fat(al) attraction: Picornaviruses Usurp Lipid Transfer at Membrane Contact Sites to Create Replication Organelles. *Trends Microbiol* 24: 535-546.

Vandesande H., Laajala M., Kantoluoto T., Ruokolainen V., Lindberg A.M. & Marjomäki V. 2020. Early entry events in Echovirus 30 infection. *J Virol* .

Vaux D., Tooze J. & Fuller S. 1990. Identification by anti-idiotype antibodies of an intracellular membrane protein that recognizes a mammalian endoplasmic reticulum retention signal. *Nature* 345: 495-502.

Wells A.I. & Coyne C.B. 2019. Enteroviruses: A Gut-Wrenching Game of Entry, Detection, and Evasion. *Viruses* 11.

Wenner H.A., Harmon P., Behbehani A.M., Rouhandeh H. & Kamitsuka P.S. 1967. The antigenic heterogeneity of type 30 echoviruses. *Am J Epidemiol* 85: 240-249.

Wu Y., Lou Z., Miao Y., Yu Y., Dong H., Peng W., Bartlam M., Li X. & Rao Z. 2010. Structures of EV71 RNA-dependent RNA polymerase in complex with substrate and analogue provide a drug target against the hand-foot-and-mouth disease pandemic in China. *Protein Cell* 1: 491-500.

Yang X., Yan Y., Weng Y., He A., Zhang H., Chen W. & Zhou Y. 2013. Molecular epidemiology of Echovirus 30 in Fujian, China between 2001 and 2011. *J Med Virol* 85: 696-702.

Zhao X., Zhang G., Liu S., Chen X., Peng R., Dai L., Qu X., Li S., Song H., Gao Z., Yuan P., Liu Z., Li C., Shang Z., Li Y., Zhang M., Qi J., Wang H., Du N., Wu Y., Bi Y., Gao S., Shi Y., Yan J., Zhang Y., Xie Z., Wei W. & Gao G.F. 2019. Human Neonatal Fc Receptor Is the Cellular Uncoating Receptor for Enterovirus B. *Cell* 177: 1553-1565.e16.

Zhao Y.N., Jiang Q.W., Jiang R.J., Chen L. & Perlin D.S. 2005. Echovirus 30, Jiangsu Province, China. *Emerging infectious diseases* 11: 562-567.

Österback R., Kalliokoski T., Lähdesmäki T., Peltola V., Ruuskanen O. & Waris M. 2015. Echovirus 30 meningitis epidemic followed by an outbreak-specific RT-qPCR. *J Clin Virol* 69: 7-11.